3008 *Chem. Mater.* **2009,** *21,* 3008–3016
DOI:10.1021/cm900965p

CHEMISTRY OF MATERIALS
Article

Characteristic Phonon Spectrum of Negative Thermal Expansion Materials with Framework Structure through Calorimetric Study of $Sc_2M_3O_{12}$ (M = W and Mo)

Yasuhisa Yamamura,* Satoaki Ikeuchi, and Kazuya Saito

Department of Chemistry, Graduate School of Pure and Applied Sciences, University of Tsukuba, Tsukuba, Ibaraki 305-8571, Japan

Received April 7, 2009. Revised Manuscript Received May 20, 2009

To study the relation between the structural characteristics and the phonon property in the negative thermal expansion (NTE) compounds, the heat capacities of $Sc_2W_3O_{12}$ and $Sc_2Mo_3O_{12}$ were measured. Spectrum analysis of heat capacity provided their effective phonon densities of states (DOS). The DOS of $Sc_2W_3O_{12}$ shows three features; low-energy phonon modes with negative mode-Grüneisen parameter (γ_i) around 5 meV, high-energy phonon modes, and separation of phonon DOS into two regions with a wide gap. The relative contribution of $\gamma_i C_i$, where C_i is heat capacity of each vibrational mode i, reveals that the low-energy phonon modes with negative γ_i cause the NTE and that the latter two features are necessary to maintain the NTE in a wide temperature range. $Sc_2Mo_3O_{12}$ has the low-energy mode with the negative γ_i. This fact indicates that $Sc_2Mo_3O_{12}$ potentially has the NTE property even in its low-temperature phase showing positive thermal expansion. A comparison of the phonon DOS with other oxides shows that the phonon features are common in the NTE oxides and related to their common chemical and structural characteristics, "strong bond" and "framework structure". This finding gives us an important guide to search for new actual and/or potential NTE compounds.

1. Introduction

A lot of negative thermal expansion (NTE) materials, which show thermal contraction with increasing temperature, have been investigated since the report[1] of the isotropic NTE material, ZrW_2O_8. The NTE materials are very important for control of thermal expansion coefficients of materials to avoid their destruction by thermal shock. The NTE materials have been found not only in oxides but also metal complexes, e.g., cyanide.[2,3] This suggests that various compounds have a possibility of the NTE property. To find and modify the potential NTE compounds makes it possible to design a new NTE compound, leading to applications of the NTE materials into various fields.

Typical NTE compounds found in the past decade include $Zr(Hf)W_2O_8$,[1,4,5] $Zr(Hf)V_2O_7$,[6,7] $A_2B_3O_{12}$ (A = trivalent cation; B = W or Mo),[8−13] NZP,[14] and cyanides.[2,3] These compounds possess two common characteristics; "strong bond" and "framework structure". For example, ZrW_2O_8 shows the strong bonds between metal (Zr, W) and oxygen atoms (M−O bond) and a framework structure composed of ZrO_6 octahedra and WO_4 tetrahedra through Zr−O−W bridges.[1] These structural characteristics yield "low-energy phonon modes" (translational and librational vibrations of the polyhedra), leading to the NTE properties of ZrW_2O_8.[15−23] Therefore, most studies of the mechanism

*Corresponding author. E-mail: yasu@chem.tsukuba.ac.jp.

(1) Mary, T. A.; Evans, J. S. O.; Vogt, T.; Sleight, A. W. *Science* **1996**, *272*, 90.
(2) Margadonna, S.; Prassides, K.; Fitch, A. N. *J. Am. Chem. Soc.* **2004**, *126*, 15390.
(3) Chapman, K. W.; Chupas, P. J.; Kepert, C. J. *J. Am. Chem. Soc.* **2005**, *127*, 15630.
(4) Martinek, C.; Hummel, F. A. *J. Am. Ceram. Soc.* **1968**, *51*, 227.
(5) Yamamura, Y.; Nakajima, N.; Tsuji, T. *Phys. Rev. B* **2001**, *64*, 184109.
(6) Korthuis, V.; Khosrovani, N.; Sleight, A. W. *Chem. Mater.* **1995**, *7*, 412.
(7) Turquat, C.; Muller, C.; Nigrelli, E.; Leroux, C.; Soubeyroux, J.-L.; Nihoul, G. *Eur. Phys. J. AP* **2000**, *10*, 15.
(8) Evans, J. S. O.; Mary, T. A.; Sleight, A. W. *J. Solid State Chem.* **1997**, *133*, 580.
(9) Evans, J. S. O.; Mary, T. A.; Sleight, A. W. *Physica B* **1998**, *241−243*, 311.
(10) Forster, P. M.; Yokochi, A.; Sleight, A. W. *J. Solid State Chem.* **1998**, *140*, 157.
(11) Forster, P. M.; Sleight, A. *Int. J. Inorg. Mater.* **1999**, *1*, 123.
(12) Tyagi, A. K.; Achary, S. N.; Mathews, M. D. *J. Alloys Compd.* **2002**, *339*, 207.
(13) Sumithra, S.; Tyagi, A. K.; Umarji, A. M. *Mater. Sci. Eng., B* **2005**, *116*, 14.
(14) Roy, R.; Agrawal, D. K.; McKinstry, H. A. *Annu. Rev. Mater. Sci.* **1989**, *19*, 59.
(15) Ramirez, A. P.; Kowach, G. R. *Phy. Rev. Lett.* **1998**, *80*, 4903.
(16) Ernst, G.; Broholm, C.; Kowach, G. R.; Ramirez, A. P. *Nature (London)* **1998**, *396*, 147.
(17) David, W. I. F.; Evans, J. S. O.; Sleight, A. W. *Europhys. Lett.* **1999**, *46*, 661.
(18) Mittal, R.; Chaplot, S. L. *Phys. Rev. B* **1999**, *60*, 7234.
(19) Mittal, R.; Chaplot, S. L.; Schober, H.; Mary, T. A. *Phys. Rev. Lett.* **2001**, *86*, 4692.
(20) Yamamura, Y.; Nakajima, N.; Tsuji, T.; Koyano, M.; Iwasa, Y.; Katayama, S.; Saito, K.; Sorai, M. *Phys. Rev. B* **2002**, *66*, 014301.
(21) Cao, D.; Bridges, F.; Kowach, G. R.; Ramirez, A. P. *Phys. Rev. Lett.* **2002**, *89*, 215902.
(22) Hancock, J. N.; Turpen, C.; Schlesinger, Z.; Kowach, G. R.; Ramirez, A. P. *Phys. Rev. Lett.* **2004**, *93*, 225501.
(23) Tucker, M. G.; Goodwin, A. L.; Dove, M. T.; Keen, D. A.; Wells, S. A.; Evans, J. S. O. *Phys. Rev. Lett.* **2005**, *95*, 25501.

Published on Web 06/11/2009

of the NTE have dealt with the low energy phonon modes so far. Only the presence of such low-energy phonon modes is, however, insufficient as a guide to find new actual and/or potential NTE compounds, because all compounds having such low energy phonon modes do not exhibit the NTE property. It is, therefore, very important to identify other features of lattice vibration originating in the structural characteristics.

To know the characteristic phonon features of the NTE materials, we will discuss the following two subjects in this paper. One is phonon properties of $Sc_2W_3O_{12}$ and $Sc_2Mo_3O_{12}$ through measurements of their heat capacities. $A_2B_3O_{12}$ (A and B = trivalent and quadrivalent cations) is a large family of compounds and consists of a corner-sharing network of AO_6 octahedra and BO_4 tetrahedra, similarly to the framework structure of ZrW_2O_8. Because $Sc_2W_3O_{12}$,[8,9,24] $Y_2W_3O_{12}$,[11] and $Lu_2W_3O_{12}$[10] show the NTE properties in a wide temperature range, the family has been investigated so far. $Sc_2W_3O_{12}$ and $Sc_2Mo_3O_{12}$ are two typical compounds in the family. $Sc_2W_3O_{12}$ shows the NTE over a temperature range of 10 to 1073 K.[24] The crystal structure of $Sc_2W_3O_{12}$ is of orthorhombic (*Pnca*). The *a* and *c* cell parameters decrease with increasing temperature, while the *b* cell parameter increases. The unit-cell volume decreases with increasing temperature in the whole temperature. The other compound, $Sc_2Mo_3O_{12}$, also shows the orthorhombic phase (*Pnca*) and the NTE at room temperature.[25] However, the compound undergoes a structural phase transition at about 178 K.[25] At the phase transition temperature, the volume reduces with going from the high-temperature to low-temperature phases. The low temperature phase is monoclinic ($P2_1/a$) and shows a positive thermal expansion, though the framework structure with the polyhedra is maintained.[25] The low-temperature phase of $Sc_2Mo_3O_{12}$ is thus characterized as the potential NTE compound into which the NTE property emerges upon the phase transition. A comparison of the phonon properties between $Sc_2W_3O_{12}$ and $Sc_2Mo_3O_{12}$ will thus provide us a key factor for emergence of the NTE properties.

The second object of this paper is the survey of the phonon properties of NTE compounds with framework structures. A lot of experimental and theoretical papers have reported the phonon spectra of various NTE compounds so far. It is expected that a comparison of those phonon spectra makes it possible to pick up a common structural and phonon features of the NTE compounds. Although the rigid unit modes (RUMs) model[26] has been proposed for a limited class of the framework structure materials, the model cannot be applied to all NTE materials with the framework structure, e.g., the $A_2B_3O_{12}$ family has no RUM although it shows the NTE.[27] In this paper, we study the phonon densities of states of $Sc_2W_3O_{12}$ and $Sc_2Mo_3O_{12}$, and the structural and phonon features common to the NTE compounds will be identified through the comparison of the phonon properties of various NTE compounds.

2. Experimental Section

$Sc_2Mo_3O_{12}$ and $Sc_2W_3O_{12}$ were synthesized by conventional solid-state reactions. Sc_2O_3 (99.9% Soekawa) and MoO_3 (99.99% Kojund) or WO_3 (99.99% Kojund) were mixed and pressed into pellets. The pellets were sintered at 1373 K for 12 h in air. X-ray diffraction at room temperature confirmed that both the synthesized compounds were of single phase. The samples for calorimetry were sealed in a gold-plated copper calorimeter vessel with helium under atmospheric pressure. The masses of the samples were 9.7249 g (17.069 mmol) for $Sc_2Mo_3O_{12}$ and 15.6419 g (18.7682 mmol) for $Sc_2W_3O_{12}$ after the buoyancy correction. The two working thermometers mounted on the calorimeter vessel were a platinum resistance thermometer (Minco, S1059) for the use from 13.8 to 330 K and a germanium resistance thermometer (Lake-Shore, GR-200B500) from 4.2 to 13.8 K. Their temperature scales are based upon the ITS-90. The details of the adiabatic calorimeter used and its operations are described elsewhere.[28] The measurement was carried out by the so-called intermittent heating adiabatic method. The temperature increment by a single energy input (Joule heating) was less than 1% of temperature. After energy input was turned off, thermal equilibrium inside the vessel was attained within a normal time (1−10 min depending on temperature) outside the temperature region near phase transitions. Each sample contributed more than 20% at all temperatures to the total heat capacity including that of the calorimeter vessel. Heat capacities of the samples were measured in the temperature region from 20 K down to 1.8 K using a commercial relaxation calorimeter (PPMS, Quantum Design). Each sample (18.1 mg for $Sc_2Mo_3O_{12}$ and 20.2 mg for $Sc_2W_3O_{12}$) was adhered to the sample holder with Apiezon-N grease.

3. Results and Discussion

3.1. Heat Capacities and Phonon Properties of $Sc_2W_3O_{12}$ and $Sc_2Mo_3O_{12}$. *3.1.1. Heat Capacity and Phase Transition of $Sc_2Mo_3O_{12}$.* Heat capacity (C_p) of $Sc_2Mo_3O_{12}$ was measured from 1.8 to 310 K as shown in Figure 1. The result shows a sharp anomaly at 178 K. Because the temperature of the anomaly corresponds to that of the jump of the cell volume of $Sc_2Mo_3O_{12}$, the anomaly is attributed to the structural phase transition between monoclinic and orthorhombic phases.[25] Figure 2 shows an enlarged plot of heat capacity of $Sc_2Mo_3O_{12}$ around 180 K. The filled plots measured after cooling down to 150 K from 200 K exhibits a supercooling phenomenon. This indicates that the phase transition is of first order. To separate the excess heat capacity, a baseline was determined as shown by a solid curve in Figure 2. The measured supercooling curve was adopted as the baseline above the phase transition temperature (T_{trs} = (178 ± 1) K). The baseline below the T_{trs} was determined by extrapolation of heat capacities from

(24) Evans, J. S. O.; Mary, T. A.; Sleight, A. W. *J. Solid State Chem.* **1998**, *137*, 148.
(25) Evans, J. S. O.; Mary, T. A. *Int. J. Inorg. Mater.* **2000**, *2*, 143.
(26) Hammonds, K. D.; Dove, M. T.; Giddy, A. P.; Heine, V.; Winkler, B. *Am. Mineral.* **1996**, *81*, 1057.
(27) Tao, J. Z.; Sleight, A. W. *J. Solid State Chem.* **2003**, *173*, 442.
(28) Yamamura, Y.; Saito, K.; Saitoh, H.; Matsuyama, H.; Kikuchi, K.; Ikemoto, I. *J. Phys. Chem. Solids* **1995**, *56*, 107.

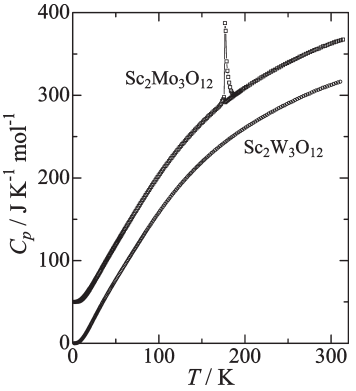

Figure 1. Heat capacities of $Sc_2W_3O_{12}$ (circle) and $Sc_2Mo_3O_{12}$ (square). The heat capacity of $Sc_2Mo_3O_{12}$ is shifted upward by 50 J K^{-1} mol^{-1}.

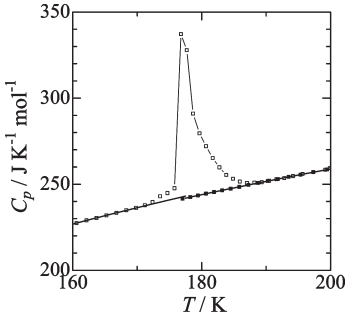

Figure 2. Enlarged plot of heat capacity of $Sc_2Mo_3O_{12}$ around 180 K. Filled squares indicate the heat capacity of the supercooled orthorhombic phase. A solid line is a normal heat capacity to separate excess heat capacity.

140 to 165 K. The resultant excess heat capacities were integrated over the temperature region from 165 to 190 K to yield enthalpy ($\Delta_{trs}H$) and entropy ($\Delta_{trs}S$) of transition. The $\Delta_{trs}H$ and $\Delta_{trs}S$ thus determined are (356 ± 5) J mol^{-1} and (2.01 ± 0.5) J K^{-1} mol^{-1}, respectively. These values are slightly larger than those of the previous DSC results.[29] The $\Delta_{trs}S$ is much smaller than Rln 2 (≈ 5.8 J K^{-1} mol^{-1}, R is gas constant), which is the $\Delta_{trs}S$ value of a typical order−disorder transition. This fact supports that this phase transition is not an order−disorder type but displacive one as suggested previously.[25,29] Many members of $A_2B_3O_{12}$ undergo a structural phase transition between monoclinic and orthorhombic phases.[8,12,25,29−32] Their $\Delta_{trs}S$ are nearly the same as that of $Sc_2Mo_3O_{12}$. It is thus suggested that the monoclinic-to-orthorhombic phase transitions of $A_2B_3O_{12}$ type compounds are of displacive type.

3.1.2. Heat Capacities of $Sc_2W_3O_{12}$ and $Sc_2Mo_3O_{12}$. Heat capacity of $Sc_2W_3O_{12}$ was measured from 1.8 to 310 K as shown in Figure 1. No anomaly is observed in the whole temperature range, in contrast to $Sc_2Mo_3O_{12}$. This fact implies that the orthorhombic phase of $Sc_2W_3O_{12}$ is kept even at low temperatures. The C_p of $Sc_2W_3O_{12}$ is larger than that of $Sc_2Mo_3O_{12}$. Figure 3 shows the C_pT^{-3} plots of $Sc_2W_3O_{12}$ and $Sc_2Mo_3O_{12}$ against log T. Their curves commonly show a constant C_pT^{-3} in a narrow temperature region below about 3 K and a large peak at 10 K. The constant C_pT^{-3} values in the lowest temperature region differs notably between $Sc_2W_3O_{12}$ and

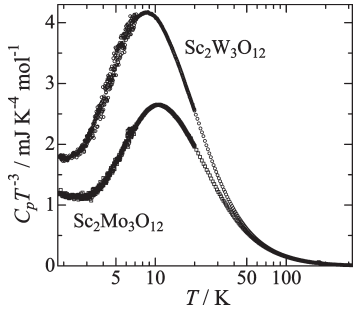

Figure 3. C_pT^{-3} of $Sc_2W_3O_{12}$ (circle) and $Sc_2Mo_3O_{12}$ (square) for the sake of comparison.

$Sc_2Mo_3O_{12}$. From the constant C_pT^{-3} values, the Debye temperatures (Θ_D) of $Sc_2W_3O_{12}$ and $Sc_2Mo_3O_{12}$ are calculated to be 265 and 309 K, respectively, assuming 51 (17 × 3) degrees of freedom per formula unit.

Optical phonon modes approximated well by the Einstein model give a bell-shaped peak in the C_pT^{-3} plot. For ZrW_2O_8 type compounds, many previous works[15,20,33−37] have revealed that the bell-shaped peak in C_pT^{-3} is crucial for the NTE of these compounds, because the low-energy modes associated with the large peak in C_pT^{-3} often have negative mode-Grüneisen parameters. As the bell-shaped peak is also seen in $Sc_2W_3O_{12}$ and $Sc_2Mo_3O_{12}$, it is natural to say that the low-energy Einstein modes contribute to heat capacity in the present cases. The peak of $Sc_2W_3O_{12}$ is at a slightly lower temperature than that of $Sc_2Mo_3O_{12}$. The height of the peak for $Sc_2W_3O_{12}$ is remarkably larger than that of $Sc_2Mo_3O_{12}$. These differences strongly imply that distributions of the low-energy optical phonon modes, which affect the NTE property, differ significantly between the two compounds. We then evaluate their phonon distributions and mode-Grüneisen parameters from the heat capacities in the following sections.

3.1.3. Effective Phonon Density of States and Mode-Grüneisen Parameter of $Sc_2W_3O_{12}$. Heat capacity of ZrW_2O_8 was analyzed first by Ramirez and Kowach,[15] leading to the identification of low-energy phonon modes around 5 meV in addition to acoustic modes described by the Debye and Einstein functions. In their method, a few Debye functions with high characteristic temperatures describe most of heat capacity of the crystal. Although the method facilitated the detection of the characteristic low-frequency Einstein modes, it was difficult to express

(29) Varga, T.; Moats, J. L.; Ushakov, S. V.; Navrotsky, A. *J. Mater. Res.* **2007**, *22*, 2512.
(30) Nassau, K.; Levinstein, H. J.; Loiacono, G. M. *J. Am. Ceram. Soc.* **1964**, *47*, 363.
(31) Nassau, K.; Levinstein, H. J.; Loiacono, G. M. *J. Phys. Chem. Solids* **1965**, *26*, 1805.
(32) Sleight, A. W.; Brixner, L. H. *J. Solid State Chem.* **1973**, *7*, 172.
(33) Yamamura, Y.; Nakajima, N.; Tsuji, T.; Iwasa, Y.; Saito, K.; Sorai, M. *Solid State Commun.* **2002**, *121*, 213.
(34) Yamamura, Y.; Nakajima, N.; Tsuji, T.; Koyano, M.; Iwasa, Y.; Katayama, S.; Saito, K.; Sorai, M. *J. Ceram. Soc. Jpn., Suppl.* **2004**, *112−1*, S291.
(35) Yamamura, Y.; Saito, K. *J. Phys. Soc. Jpn.* **2007**, *76*, 123603.
(36) Boerio-Gotes, J.; Stevens, R.; Lang, B.; Woodfield, B. F. *J. Therm. Anal. Calorim.* **2002**, *69*, 773.
(37) Kennedy, C. A.; White, M. A.; Wilkinson, A. P.; Varga, T. *Phys. Rev. B* **2007**, *75*, 224302.

a complex and continuous frequency distribution of lattice vibrations. Besides, the method is unsuitable to discuss the frequency distribution in a high-frequency region. To describe the continuous distribution, Kieffer[38] introduced a rectangular function (R), as exemplified in Figure 5, besides the Debye (D) and Einstien (E) ones. Although the rectangular function has no clear physical meaning in contrast to the Debye and Einstein functions, the function can easily describe a wide and continuous frequency distribution of lattice vibrations, which is often seen in actual phonon density of states (DOS). The advantage of the Kieffer model has been ascertained by a lot of phonon DOS studies of a wide variety of oxides and minerals.[38−40] We could also deduce an effective phonon DOS of ZrW_2O_8 and HfW_2O_8,[20,33] and their solid solutions[34] from the heat capacities at low temperature by using the Kieffer model.

Now, the phonon DOS of $Sc_2W_3O_{12}$ is estimated from its heat capacities from 1.8 to 310 K through the spectrum analysis using the Kieffer model. Before the analysis, we need to estimate the heat capacity at constant volume, C_v, of $Sc_2W_3O_{12}$. The measured C_p data were converted to C_v by a thermodynamic relation $C_p - C_v = VT\beta^2B_T$, where V is molar volume, T temperature, β coefficient of volume expansion, and B_T isothermal bulk modulus. B_T of $Sc_2W_3O_{12}$ was reported to be 31 GPa at room temperature by Varga et al.[41] Because the temperature dependence of B_T is small below room temperature,[42] B_T is assumed to be independent of temperature in this study. The experimental values of V of $Sc_2W_3O_{12}$ at various temperatures from 10 to 450 K were taken from ref 24. The reported V increases monotonously with the decrease in temperature, but is almost constant below 50 K.[24] For this analysis, the reported V above 50 K was fitted to a function ($V(T) = aT^3 + bT + c$) by using a least-squares method. Below 50 K, a smoothed curve was estimated from the reported data. The β was calculated by differentiating the obtained molar volume curve.

The unit cell of $Sc_2W_3O_{12}$ contains four formula units, i.e., 68 (17×4) atoms.[43] There are 204 modes of lattice vibrations. We here treat only 3 out of 204 modes as acoustic modes. This treatment assumes that only the "acoustic modes" within the first Brillouin zone are acoustic modes, whereas similar modes folded by the zone boundary are classified as "optical modes". The total number of optical modes including such "optical modes" is thus 201 per unit cell. The Debye function is assigned to the acoustic modes with the Debye temperature (64.9 K) calculated from the low temperature limit in the C_pT^{-3} plot against log T (Figure 4b) assuming 3 degrees of freedom per 4 formula units (0.75 degrees of freedom per 1 formula unit). The degrees of freedom assigned to each function and their characteristic temperatures were determined by using a nonlinear least-squares method. Some trials showed that at least four Einstein (E1, E2, E3, E4) and two rectangular (R1, R2) functions besides one Debye function (D) were necessary for good fit.

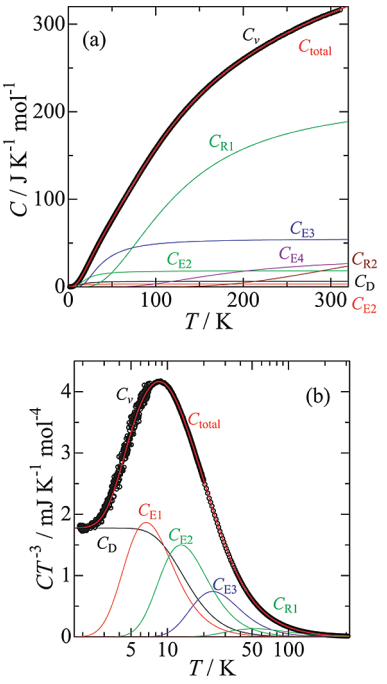

Figure 4. Heat-capacity contributions of seven functions (C_D, C_{E1}, C_{E2}, C_{E3}, C_{E4}, C_{R1}, C_{R2}), their sum ($C_{total} = \Sigma C_i$), and C_v obtained from the experimental heat-capacity for $Sc_2W_3O_{12}$ in the $C-T$ (a) and $CT^{-3}-\log T$ (b) forms.

Table 1. Parameters from the Analysis of Heat Capacities for $Sc_2W_3O_{12}$ and $Sc_2Mo_3O_{12}$

$A_2B_3O_{12}$	mode	degrees of freedom per 1 formula unit	Θ (K)	γ_i
$Sc_2W_3O_{12}$	D	0.75	64.9	1.0
	E1	0.374	32.9	−12
	E2	2.19	63.8	−1.0
	E3	6.58	116	0.18
	E4	4.18	587	0.03
	R1	25.8	178−591	0.001
	R2	11.2	1221−1552	0.11
$Sc_2Mo_3O_{12}$	D	0.375	60.2	0.78
	E1	0.277	37.9	2.0
	E2	1.84	65.1	−2.0
	E3	5.03	113	1.2
	E4	4.71	591	3.4
	R1	27.7	148−591	0.39
	R2	11.1	1226−1510	17

The result of fit for $Sc_2W_3O_{12}$ is shown in Figure 4, where each heat capacity contribution of those seven functions C_i and their sum ($C_{total} = \Sigma C_i$) are plotted together with the corrected experimental C_v. The C_{total} agrees very well with the experimental C_v. The contribution of C_{R1} is the largest below 300 K. The parameters determined for $Sc_2W_3O_{12}$ are summarized in Table 1. The corresponding effective phonon DOS is shown in Figure 5. The effective DOS is distributed below 1552 K, which is the highest characteristic temperature in this

(38) Kieffer, S. W. *Rev. Geophys. Space Phys.* **1979**, *17*, 35.
(39) Ross, N. L. In The Stability of Minerals; Price G. D., Ross. N. L., Eds.; Chapman & Hall: London, 1993; Chapter 4.
(40) Navrotsky, A. Physics and Chemistry of Earth Materials; Cambridge University Press: New York, 1994; Chapter 6.
(41) Varga, T; Wilkinson, A. P.; Lind, C.; Bassett, W. A.; Zha, C.-S. *Phys. Rev. B* **2005**, *71*, 214106.
(42) Anderson, O. L. Equations of State of Solids for Geophysics and Ceramic Sience; Oxford University Press: New York, 1995.
(43) Abrahams, S. C.; Bernstein, J. L. *J. Chem. Phys.* **1966**, *45*, 2745.

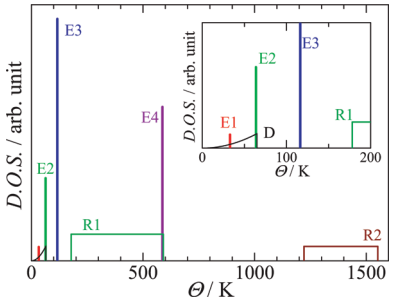

Figure 5. Effective phonon DOS of $Sc_2W_3O_{12}$.

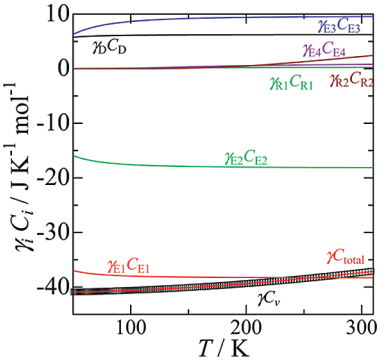

Figure 6. Temperature dependences of $\gamma_i C_i$ of $Sc_2W_3O_{12}$, where γ_i are mode-Grüneisen parameters.

analysis. This upper limit is consistent with the reported Raman and IR results,[44,45] which show the highest mode at 1021 cm^{-1} (1469 K). The effective DOS is divided into two groups. There is a wide gap from 591 to 1221 K between R1 and R2. This wide gap is also fully consistent with the reported Raman and IR results,[44,45] which show the wide gap from 385 cm^{-1} (554 K) to 801 cm^{-1} (1152 K). It is therefore reasonable to assume that the obtained effective DOS reflects a feature of the true phonon DOS of $Sc_2W_3O_{12}$ well. According to the previous spectroscopic studies[44,46] on $Sc_2W_3O_{12}$ type structure, the low-frequency modes (D, E1, E2, E3, E4, and R1) below the band gap are roughly attributed to a group of acoustic, lattice, translational, librational, and bending modes, whereas high-frequency group (R2) includes stretching modes of W−O. The stretching modes in the higher-energy region reflect the strong bonding of M−O bonds and bring the characteristic wide gap in the phonon DOS. Considering the energy region, the bending modes correspond to the E4 and R1 (partially including the lattice modes) modes and the lattice modes (translational and librational modes) to the E1, E2, and E3 modes. The C_i and C_{total} are plotted as CT^{-3} vs T in Figure 4b. It is clear that the bell-shaped peak at about 8.5 K mainly results from the $C_{E1}T^{-3}$ and $C_{E2}T^{-3}$.

The Grüneisen function[47,48] γ is given by $\gamma = (\beta B_T V/C_v)$. The γ can be expressed as a heat-capacity weighted average of mode-Grüneisen parameters[47,48] γ_i of the ith vibrational mode, i.e., $\gamma = (\Sigma\gamma_i C_i/\Sigma C_i)$, where C_i is the contribution of each vibrational mode i to heat capacity. Because of C_v, C_i, V, $B_T > 0$, the NTE compounds with $\beta < 0$ require negative γ_i. Thus, the modes with the negative γ_i are intrinsically related to the mechanism of NTE. The negative γ_i arises from the so-called tension effect,[49] which is due to large amplitude of transverse vibration of adjoining two atoms with a rigid bond. This effect yields the NTE in materials having rigid bond and framework structure composed of polyhedra.[50] Indeed, the NTE properties of ZrW_2O_8 and HfW_2O_8[20,33] originate in the low-energy phonon modes with the large negative γ_i below 8 meV, which are assigned to the translational and librational modes of their polyhedra.[15−20,33] It is then expected that the low-energy modes of $Sc_2W_3O_{12}$ have negative mode-Grüneisen parameters.

To consider the contribution of each mode to the NTE property of $Sc_2W_3O_{12}$, we estimated the mode-Grüneisen parameters from the C_i and C_v, as follows. From the fitted function $V(T)$, we can obtain the Grüneisen function $\gamma(T)$ of $Sc_2W_3O_{12}$ using the equation $\gamma = (\beta B_T V/C_v)$. Each mode-Grüneisen parameter γ_i was determined by using a nonlinear least-squares method above 50 K. The obtained γ_i values are summarized in Table 1. The negative mode-Gruneisen parameters are found for the E1 and E2 modes. The E1 and E2 modes with the negative γ_i are probably assigned to the librational one of the constituent polyhedra. The γ_{E1} shows particularly large absolute value ($\gamma_{E1} = -12$) and is of the same order as those of the low-energy modes of ZrW_2O_8 and HfW_2O_8.[20,33]

The presence of the negative γ_i is one of the requirements for the NTE. The γ ($= \beta B_T V/C_v$), however, is not always negative even if there are modes with negative γ_i. If the $|\Sigma\gamma_i C_i|$ of the modes with $\gamma_i < 0$ is smaller than that of the ones with $\gamma_i > 0$, γ can be positive. The magnitude of the $\Sigma\gamma_i C_i$ of the negative γ_i modes is therefore very important for the NTE. Figure 6 shows the results of the fit in terms of $\gamma_i C_i$. The figure clearly shows that the contributions of the E1 and E2 modes are dominant in the whole temperature range, whereas the contributions of the others below the band gap (591−1221 K) are minor. The γC_v increases with increasing temperature above 200 K and its temperature dependence is similar to that of the $\gamma_{R2}C_{R2}$. This means that the increase of the γC_v mainly comes from that of the $\gamma_{R2}C_{R2}$. On the other hand, the positive contribution of the $\gamma_{R2}C_{R2}$ is very small below room temperature, though there are 20% of all phonon modes in the R2. This is due to the wide band gap between 591 and 1221 K. If there is no band gap, the contribution of R2 to the NTE may be unnegligible even below room temperature. The band gap in the phonon

(44) Maczka, M.; Hermanowicz, K.; Hanuza, J. *J. Mol. Struct.* **2005**, *744−747*, 283.
(45) Garg, N.; Murli, C.; Tyagi, A. K.; Sharma, S. M. *Phys. Rev. B* **2005**, *72*, 064106.
(46) Ravindran, T. R.; Sivasubramanian, V.; Arora, A. K. *J. Phys.: Condens. Matter* **2005**, *17*, 277.
(47) Barron, T. H. K.; White, G. K. Heat Capacity and Thermal Expansion at Low Temperatures; Kluwer Academic: New York, 1999.
(48) Barron, T. H. K.; Collins, J. G.; White, G. K. *Adv. Phys.* **1980**, *29*, 609.
(49) Barrera, G. D.; Bruno, J. A. O.; Barron, T. H. K.; Allan, N. L. *J. Phys.: Condens. Matter* **2005**, *17*, R217.
(50) Simon, M. E.; Varma, C. M. *Phys. Rev. Lett.* **2001**, *86*, 1781.

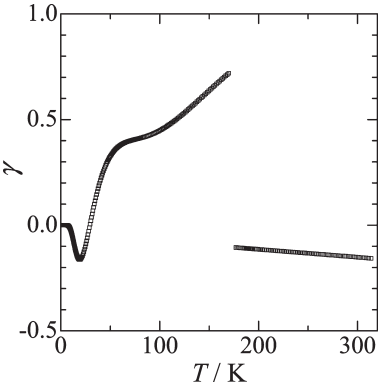

Figure 7. Grüneisen functions of $Sc_2Mo_3O_{12}$.

DOS of $Sc_2W_3O_{12}$ thus plays an important role to keep the NTE property over a wide temperature range.

3.1.4. Effective Phonon Density of States of Monoclinic Phase of $Sc_2Mo_3O_{12}$. The deduction of effective phonon DOS and mode-Grüneisen parameters applied to $Sc_2W_3O_{12}$ yielded a successful result, as shown in the previous section. We here apply the same procedure only to the low-temperature phase of $Sc_2Mo_3O_{12}$, because $Sc_2Mo_3O_{12}$ undergoes the phase transition at 178 K. Although the B_T of the low-temperature phase is necessary for the $C_p - C_v$ correction, it has not been reported. Varga et al.[51] reported $B_T = 16$ GPa of the monoclinic phase induced by pressure at room temperature. We adopt this value because the reported transition pressure at room temperature is consistent with the estimated by Clapeyron equation using the transition quantities under ambient pressure at 178 K. We therefore use the reported B_T[51] of the pressure-induced monoclinic phase for the analysis. The B_T is assumed to be independent of temperature as in the case of $Sc_2W_3O_{12}$. Evans and Mary[25] reported the experimental cell volume of $Sc_2Mo_3O_{12}$ between 4 and 300 K. Because they presented the fitted function of the cell volume below T_{trs}, we adopt it and calculated β from its temperature derivative. The values of B_T, V, and C_v offer us the Grüneisen function $\gamma(T)$ through the equation $\gamma = (\beta B_T V/C_v)$. The resultant $\gamma(T)$ is shown in Figure 7, where for the high temperature phase the B_T is 32 GPa[51] and the V was estimated from the reported cell volume using a function ($V(T) = aT^3 + bT + c$). The $\gamma(T)$ of the high temperature phase showing the NTE feature is negative. In the low-temperature phase, the $\gamma(T)$ is negative below about 30 K, but turns into positive there and increases with increasing temperature. This behavior means a change from negative to positive thermal expansion. It is noted that anomalous behavior of $\gamma(T)$ around 60 K may be nonintrinsic and come from the imperfection of the function of the cell volume.

There are 408 modes of lattice vibrations, because the unit cell of the monoclinic phase of $Sc_2Mo_3O_{12}$ contains eight formula units with 136 (17×8) atoms.[25] We treat only 3 out of 408 modes as acoustic modes within the first

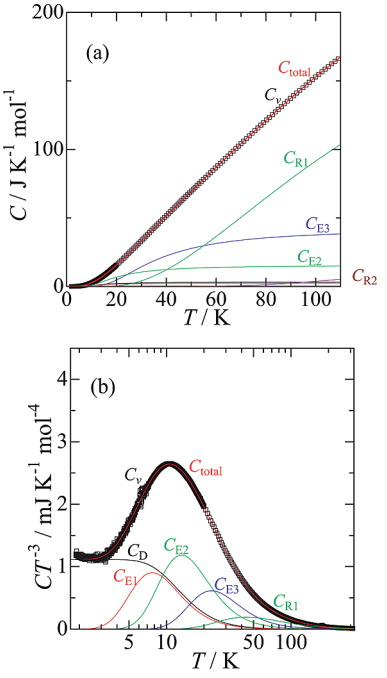

Figure 8. Heat-capacity contributions of seven functions (C_D, C_{E1}, C_{E2}, C_{E3}, C_{E4}, C_{R1}, C_{R2}), their sum ($C_{total} = \Sigma C_i$), and C_v obtained from the experimental heat-capacity for $Sc_2Mo_3O_{12}$ in the $C-T$ (a) and $CT^{-3}-\log T$ (b) forms.

Brillouin zone as in the case of $Sc_2W_3O_{12}$. The total number of optical modes is thus 405 per unit cell. The Debye function is assigned to the acoustic modes with the Debye temperature (60.2 K) calculated from the low-temperature limit in the C_pT^{-3} plot against log T (Figure 3) assuming 3 degrees of freedom per 8 formula units (0.375 degrees of freedom per 1 formula unit). The degrees of freedom assigned to each function and their characteristic temperatures were determined in the same manner as $Sc_2W_3O_{12}$. Some trials showed that at least four Einstein (E1, E2, E3, E4) and two rectangular (R1, R2) functions besides one Debye function (D) were necessary for good fit.

The result of fit for $Sc_2Mo_3O_{12}$ is shown in Figure 8. The C_{total} ($= \Sigma C_i$) coincides with the experimental C_v over the temperature region. The parameters determined are given in Table 1 together with those of $Sc_2Mo_3O_{12}$. The effective phonon DOS of $Sc_2Mo_3O_{12}$ is drawn in Figure 9. The effective phonon DOS is consistent with the Raman and IR spectra.[44,46,52,53] It is again found that the DOS is divided into two groups with a wide gap (591−1226 K). The E1 and E2 modes show that their characteristic temperatures increase slightly and their degrees of freedom decrease on going from $Sc_2W_3O_{12}$ to $Sc_2Mo_3O_{12}$. These changes result in the difference of the bell-shaped peaks between the two compounds in Figure 3.

(51) Varga, T.; Wilkinson, A. P.; Lind, C.; Bassett, W. A.; Zha, C.-S. *J. Phys.: Condens. Matter* **2005**, *17*, 4271.

(52) Paraguassu, W; Maczka, M.; Filho, A. G. S.; Freire, P. T. C.; Filho, J. M.; Melo, F. E. A.; Macklik, L.; Gerward, L.; Olsen, J. S.; Waskowska, A.; Hanuza, J. *Phys. Rev. B* **2004**, *69*, 094111.

(53) Paraguassu, W.; Maczka, M.; Filho, A. G. S.; Freire, P. T. C.; Melo, F. E. A.; Filho, J. M.; Hanuza, J. *Vibr. Spectrosc.* **2007**, *44*, 69.

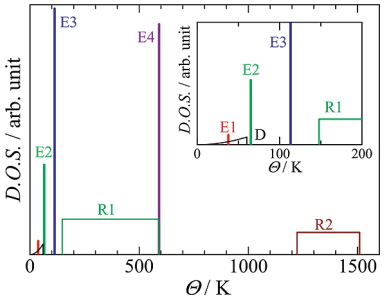

Figure 9. Effective phonon DOS of $Sc_2Mo_3O_{12}$.

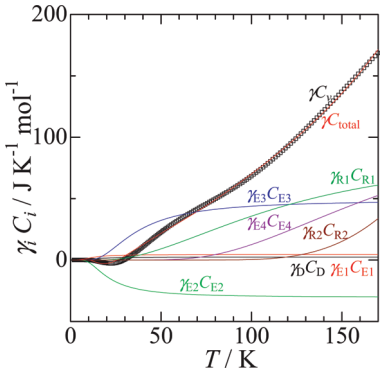

Figure 10. Temperature dependences of $\gamma_i C_i$ of $Sc_2Mo_3O_{12}$, where γ_i are mode-Grüneisen parameters.

The E1 and E2 modes have the negative mode-Grüneisen parameters in $Sc_2W_3O_{12}$. If $Sc_2Mo_3O_{12}$ potentially has the NTE property even in the low-temperature phase, the negative γ_i are expected for low-energy modes. The mode-Grüneisen parameters of $Sc_2Mo_3O_{12}$ below the T_{trs} were estimated through the same procedure as $Sc_2W_3O_{12}$. The results of the obtained γC_{total} and $\gamma_i C_i$ are plotted in Figure 10 with the experimental γC_v ($= \beta B_T V$). There is a small difference between γC_{total} and the experimental γC_v around 60 K. The small difference probably results from the nonintrinsic anomaly of γ. The obtained γ_i values are summarized in Table 1. Because the γ_{E2} is negative, the NTE can be expected. Indeed, $Sc_2Mo_3O_{12}$ shows the NTE below 30 K and has negative γ as seen in Figure 7. The contribution of $\gamma_{E2}C_{E2}$ is dominant below 30 K, resulting in the negative γ. With increasing temperature, the contribution of other modes exceed the contribution of the E2 mode, leading to the change in the sign of γ and that of β, accordingly. Consequently, the monoclinic phase of $Sc_2Mo_3O_{12}$ shows the positive thermal expansion above 30 K.

Such behavior with the sign changes of β and γ is not unique to $Sc_2Mo_3O_{12}$ but seen in a lot of NTE materials.[47,48] In contrast to $Sc_2Mo_3O_{12}$, the NTE of $Sc_2W_3O_{12}$ is kept in a wide temperature range over 1000 K because the contributions of the low energy modes (E1, E2) with the negative γ_i to γC_v are very large whereas the ones of the other modes with positive γ_i are small. This situation is also expected for the orthorhombic structure of $Sc_2Mo_3O_{12}$, because the high-temperature phase shows the NTE. That is, the NTE properties of $Sc_2W_3O_{12}$ type compounds depend strongly on their crystal structures, though these are composed of the same tetrahedra and octahedra. In the orthorhombic phase, the oxygen atoms on the corners of MoO_4 tetrahedra vibrate perpendicularly to the Sc−O−Mo bond with large amplitude, leading to the NTE of $Sc_2Mo_3O_{12}$ similarly to $Sc_2W_3O_{12}$,[9,24,54] because the large amplitude of transverse vibration results in the negative γ_i by the tension effect.[49] On the other hand, the previous structural investigation[25] revealed that the cell volume of $Sc_2Mo_3O_{12}$ becomes smaller with distorting the MoO_4 tetrahedron upon going from the orthorhombic to the monoclinic phases. In the monoclinic phase, the distortion of the MoO_4 tetrahedron suppress the vibration of the oxygen atoms on the corners and the large amplitude of transverse vibration is frozen-in.[25] Then, the suppression of the transverse vibration brings the decrease in absolute value of the negative γ_i and loweres the relative contribution of $\gamma_i C_i$ with $\gamma_i < 0$, resulting in $\gamma C_v > 0$ by contributions of $\gamma_i C_i$ with $\gamma_i > 0$. In this context, it can be said that the undistorted tetrahedron is very important for the NTE of $Sc_2W_3O_{12}$ type compounds.

$Sc_2Mo_3O_{12}$ potentially has the NTE property even in the low-temperature phase, because it has the low-energy mode with the negative γ_i. In $Sc_2Mo_3O_{12}$, the potential of the NTE property is drawn out by the phase transition from the monoclinic to orthorhombic phases. It is, however, possible to bring out such a potential NTE property by not only a phase transition but also a chemical modification. The change from $Sc_2Mo_3O_{12}$ to $Sc_2W_3O_{12}$ can be regarded as one of such examples. $A_2B_3O_{12}$ compounds can accommodate a variety of cations at A site and provide various NTE coefficients and phase transition temperatures.[8] $In_2W_3O_{12}$ undergoes the monoclinic-to-orthorhombic phase transition at T_{trs} = 500 K[32,55,56] and shows the NTE above T_{trs}.[55,56] That is, the $In_2W_3O_{12}$ is a potential NTE compound. It was reported that $InAl(WO_4)_3$, in which In is substituted for Al by 50%, shows zero thermal expansion in a wide temperature range from 300 to 800 K.[55] This fact suggests that we have a possibility to find new NTE compounds in $Sc_2W_3O_{12}$ type compounds through a chemical modification of a compound having the potential NTE property. This may be also applicable to other compounds with such framework structure. To seek the new compounds with actual or potential NTE properties, it is necessary to reveal the relation between the chemical and structural features and the phonon properties in the NTE compounds. We survey the phonon properties of the NTE compounds with the framework structure in the next section.

3.2. Characteristic Phonon Spectrum of NTE materials with Framework Structure. Both $Sc_2W_3O_{12}$ and $Sc_2Mo_3O_{12}$ have the features of "strong bond" and "framework structure". These structural features are reflected in their characteristic phonon properties revealed by the spectral analyses of heat capacity; low-energy phonon modes with

(54) Weller, M. T.; Henry, P. F.; Wilson, C. C. *J. Phys. Chem. B* **2000**, *104*, 1224.
(55) Evans, J. S. O. *J. Chem. Soc., Dalton Trans.* **1999**, 3317.
(56) Sivasubramanian, V.; Ravindran, T. R.; Nithya, R.; Arora, A. K. *J. Appl. Phys.* **2004**, *96*, 387.

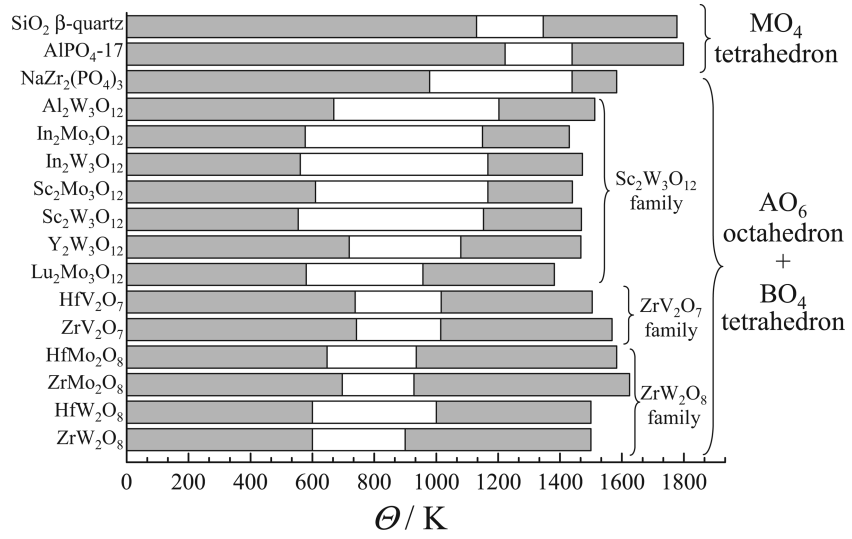

Figure 11. Phonon distributions of the reported NTE oxides with framework structure and their analogues; ZrW_2O_8,[16,20,37,57−61] ZrV_2O_7,[62−65] $Sc_2W_3O_{12}$,[44,53,65−67] NZP,[68] zeolite,[69] and silica[70−72] families. A continuous distribution is depicted as a shaded belt, whereas an open belt shows the phonon gap.

negative γ_i, high-energy phonon modes, and a gap between phonon bands. These characteristics are observed also in ZrW_2O_8,[20] which is the representative NTE compound. Besides ZrW_2O_8, there are a lot of NTE compounds, whose NTE mechanisms mainly arise from lattice dynamics. Those NTE compounds also have the features, strong bond and framework structure, in common. These common features are to be reflected in phonon properties. Here, we survey the NTE compounds reported previously and gather together their phonon properties to see possible interrelation.

The phonon properties of ZrW_2O_8 have been investigated fully and obtained from inelastic neutron scattering,[16,19] heat capacity,[15,20,36] IR and Raman spectra.[20,58,59] However, investigations are limited to spectroscopy or lattice dynamical calculation in most NTE compounds. Although the IR and Raman spectra provide only the information of phonons at Γ point in reciprocal space, the spectra reflect well a distribution of phonon. This was demonstrated by the previous work[20] of ZrW_2O_8 and HfW_2O_8 and by the present analysis of $Sc_2W_3O_{12}$ and $Sc_2Mo_3O_{12}$. The available phonon distributions of the NTE oxides with the framework structure and their analogues are summarized in Figure 11; ZrW_2O_8,[16,20,37,57−61] ZrV_2O_7,[62−65] $Sc_2W_3O_{12}$,[44,53,65−67] NZP,[68] zeolite,[69] and silica[70−72] families. In the figure, a continuous distribution is depicted as a shaded belt, whereas the open belt shows the phonon gap. All the compounds show in common two characteristics; high-energy phonon modes and separation of phonon distribution into two regions within a wide gap. The two characteristics agree well with ZrW_2O_8 and $Sc_2W_3O_{12}$.

The high-energy mode means the existence of strong bond between constituent atoms. In the case of the NTE oxides, the strong bond is the bond between metal and oxygen atoms, which form polyhedra in the crystal. The high-energy modes are then assigned to be internal modes of the polyhedra. The modes are distributed in the energy range around 1200 K (1500 cm^{-1}) for ZrW_2O_8, $Sc_2W_3O_{12}$, and ZrV_2O_7 types. These modes are, however, softer than those of SiO_2 and zeolites, because the Si−O bond of the tetrahedron is very strong. Anyway, the strong bond yields the rigid polyhedra and maintains the framework structure.

The compounds showing the NTE in a wide temperature range have the wide phonon band gap from ca. 600 K to at least about 1000 K in common. The phonon modes below the gap mainly contribute to heat capacity around room temperature. The contribution of the highest energy mode below the gap amounts to ca. 90% of the saturated classical value. The contributions of the phonon modes below the phonon gap to the Grüneisen function and the thermal expansion are saturated around room temperature, accordingly. On the other hand, the heat capacity due to the higher-energy modes above the gap is smaller than half of the saturated value. Therefore, the

(57) Evans, J. S. O.; Mary, T. A.; Vogt, T. M.; Subramanian, A.; Sleight, A. W. *Chem. Mater.* **1996**, *8*, 2809.
(58) Ravindran, T. R.; Arora, A. K.; Mary, T. A. *Phys. Rev. Lett.* **2000**, *84*, 3879.
(59) Mittal, R.; Chaplot, S. L. *Solid State Commun.* **2000**, *115*, 319.
(60) Mittal, R.; Chaplot, S. L.; Kolesnikov, A. I.; Loong, C.-K.; Mary, T. A. *Phys. Rev. B* **2003**, *68*, 054302.
(61) Mittal, R.; Chaplot, S. L.; Schober, H.; Kolesnikov, A. I.; Loong, C.-K.; Lind, C.; Wilkinson, A. P. *Phys. Rev. B* **2004**, *70*, 214303.
(62) Hemamala, U. L. C.; El-Ghussein, F.; Muthu, D. V. S.; Anderson, A. M. K.; Carlson, S.; Ouyang, L.; Kruger, M. B. *Solid State Commun.* **2007**, *141*, 680.
(63) Sakuntala, T.; Arora, A. K.; Sivasubramanian, V.; Rao, R.; Kalavathi, S.; Deb, S. K. *Phys. Rev. B* **2007**, *75*, 174119.
(64) Mittal, R.; Chaplot, S. L. *Phys. Rev. B* **2008**, *78*, 174303.
(65) Hemamala, U. L. C.; El-Ghussein, F.; Goedken, A. M.; Chen, B.; Leroux, Ch.; Kruger, M. B. *Phys. Rev. B* **2004**, *70*, 214114.
(66) Viola, M.; del, C.; Sangra, A. M.; Pedregosa, J. C. *J. Mater. Sci.* **1993**, *28*, 6587.
(67) Karmaker, S.; Deb, S. K.; Tyagi, A. K.; Sharma, S. M. *J. Solid State Chem.* **2004**, *177*, 4087.
(68) Chakir, M.; Jazouli, A. E.; de Wall, D. *J. Solid. State Chem.* **2006**, *179*, 1883.
(69) Tao, J. Z.; Sleight, A. W. *J. Phys. Chem. Solids* **2003**, *64*, 1473.
(70) Simon, I.; McMahon, H. O. *J. Chem. Phys.* **1953**, *21*, 23.
(71) Bates, J. B.; Quist, A. S. *J. Chem. Phys.* **1972**, *56*, 1528.
(72) Etchepare, J.; Merian, M.; Smetankine, L. *J. Chem. Phys.* **1974**, *60*, 1873.

contribution of those modes to the NTE property is small below room temperature, even if the modes have the positive mode-Grüneisen parameter as described in the previous section for $Sc_2W_3O_{12}$. That is, the large phonon gap reduces the contribution of the high-energy modes to the positive thermal expansion, leading to the NTE over a wide temperature range.

The wide phonon gap is closely related to the framework structure. Fei et al.[73] revealed that the phonon gap opens with increasing open space in crystal as follows: Magnesium silicon oxide, $MgSiO_3$, has various polymorphs (perovskite, ilmenite, garnet, pyroxene, and so on) and has extensively been studied so far. The garnet structure of the compound consists of tetrahedra and octahedra and has large open space inside. The open space structure shows a wide gap between 600 and 800 cm^{-1} in its phonon DOS. On the other hand, the perovskite structure has a framework composed of only octahedra with a cation (Si) at each center, and the other cations (Mg) lie at interstitials between the octahedra. The perovskite structure thus has higher density than the garnet structure. The perovskite structure has no gap in the phonon DOS. That is, the wide phonon gap is one of the features of the framework structure. In the case of the NTE oxides in Figure 11, the oxides consist of only tetrahedra or tetrahedra and octahedra, leading to open framework structures. This open framework structure results in the wide phonon gap.

The NTE compounds with the open framework structure are not limited to oxide. An organic NTE compound, strontium acetylenedicarboxylate $Sr(C_2(COO)_2)$,[74] has a metal-organic framework structure. Inorganic cyanide complexes have the framework structure with open space and show the NTE; $Zn(CN)_2$,[75,76] $Cd(CN)_2$,[75,76] and Prussian blues.[77] The NTE cyanide complexes also have the two phonon features; the high-energy modes and the wide phonon gap. $Zn(CN)_2$, for example, has the phonon gap extended from 660 to 3100 K and the high-energy modes around 3200 K assigned to the CN bond.[78,79] Such phonon features can be attributed to the framework structure and the strong bond. The CN group bridges two polyhedra in the cyanide complexes. Such a situation is also seen in $CuScO_2$,[80] which has a framework structure with the O−Cu−O linkage and shows an anisotropic NTE property. These two coordination linkages behave like dihedron with a coordination number of 2. For the NTE property, the two coordination linkage is superior to the tetrahedron (the coordination number is 4) and the octahedron (8) in bond strength and large open space around it. On the other hand, the octahedron surpasses the tetrahedron and dihedron in isotropy and flexibility to form the framework structure. The coordination number of the polyhedra is also one of the important keys to realize the NTE property.

4. Conclusion

In this study, the effective phonon DOS of $Sc_2W_3O_{12}$ and $Sc_2Mo_3O_{12}$ were obtained by the spectrum analysis of their heat capacities. These phonon DOS exhibited three phonon features; the low-energy phonon mode, the high-energy phonon mode, and the wide phonon gap. The importance of all of these features was demonstrated. The three features were found to be common to various NTE compounds. The three phonon features originated in the chemical and the structural characteristics of the NTE compounds; the strong bond and the framework structure composed of polyhedra with open space. The present study establishes a guide to search for new NTE compounds. The following three points are essential: First the compounds are to be chosen from those with the strong bond between the constituent atoms, which is indispensable to formation of a framework structure. Second, the NTE compounds need the framework structure composed of polyhedra, which yields low-energy phonon mode(s) with negative mode-Grüneiusen parameter(s) due to librational and translational modes of the polyhedra. The coordination number of the polyhedra is also important for the NTE property. Third, the framework structure must have a large open space, because the phonon gap opens and the contribution of the high-energy mode to the positive thermal expansion is reduced. The fulfillment of the three points is the minimal condition for the actual and potential NTE compounds. In this context, the minerals and the oxides with framework structure are candidates. Considering various $Sc_2W_3O_{12}$ type compounds, chemical modification such as substitution will bring out the potential NTE property.

Acknowledgment. The authors thank Professor T. Tsuji (JAIST) and Professor M. Sorai (Osaka University) for their continuing interest and encouragement. This work was supported by a Grant-in-Aid for Scientific Research (C) (19560672) from the Japan Society for the Promotion of Science (JSPS) (Y.Y.).

Supporting Information Available: Tables of standard thermodynamic quantities of $Sc_2W_3O_{12}$ and $Sc_2Mo_3O_{12}$ (PDF). This material is available free of charge via the Internet at http://pubs.acs.org.

(73) Fei, Y.; Saxena, S. K.; Navrotsky, A. *J. Geophys. Res.* **1990**, *95*, 6915.
(74) Hohn, F.; Pantenburg, I.; Ruschewitz, U. *Chem.−Eur. J.* **2002**, *8*, 4536.
(75) Williams, D. J.; Partin, D. E.; Lincoln, F. J.; Kouvetakis, J.; O'Keeffe, M. *J. Solid State Chem.* **1997**, *134*, 164.
(76) Goodwin, A. L.; Kepert, C. J. *Phys. Rev. B* **2005**, *71*, 140301(R).
(77) Margadonna, S.; Prassides, K.; Fitch, A. N. *J. Am. Chem. Soc.* **2004**, *126*, 15390.
(78) Zwanziger, J. W. *Phys. Rev. B* **2007**, *76*, 052102.
(79) Ravindran, T. R.; Arora, A. K.; Chandra, S.; Valsakumar, M. C.; Shekar, N. V. C. *Phys. Rev. B* **2007**, *76*, 054302.
(80) Li, J.; Yokochi, A.; Amos, T. G.; Sleight, A. W. *Chem. Mater.* **2002**, *14*, 2602.